

Observational templates of star cluster disruption

The stellar group NGC 1901 in front of the Large Magellanic Cloud

G. Carraro^{1,2}, R. de la Fuente Marcos³, S. Villanova¹, C. Moni Bidin², C. de la Fuente Marcos³, H. Baumgardt⁴, and G. Solivella⁵

¹Dipartimento di Astronomia, Università di Padova, Vicolo Osservatorio 2, I-35122 Padova, Italy

²Departamento de Astronomía, Universidad de Chile, Casilla 36-D, Santiago, Chile

³Suffolk University Madrid Campus, C/ Viña 3, E-28003 Madrid, Spain

⁴AIfA, University of Bonn, Auf dem Hügel 71, D-53121 Bonn, Germany

⁵Facultad de Ciencias Astronómicas y Geofísicas de la UNLP, IALP-CONICET, Paseo del Bosque s/n, La Plata, Argentina

Received November 1, 2006; accepted XXXXXXXX XX, XXXX

ABSTRACT

Context. Observations indicate that present-day star formation in the Milky Way disk takes place in stellar ensembles or clusters rather than in isolation. Bound, long lived stellar groups are known as open clusters. They gradually lose stars and in their final evolutionary stages they are severely disrupted leaving an open cluster remnant made of a few stars.

Aims. In this paper, we study in detail the stellar content and kinematics of the poorly populated star cluster NGC 1901. This object appears projected against the Large Magellanic Cloud. The aim of the present work is to derive the current evolutionary status, binary fraction, age and mass of this stellar group. These are fundamental quantities to compare with those from N -body models in order to study the most general topic of star cluster evolution and dissolution.

Methods. The analysis is performed using wide-field photometry in the UBVI pass-band, proper motions from the UCAC.2 catalog, and 3 epochs of high resolution spectroscopy, as well as results from extensive N -body calculations.

Results. The star group NGC 1901 is found to be an ensemble of solar metallicity stars, 400 ± 100 Myr old, with a core radius of 0.23 pc, a tidal radius of 1.0 pc, and located at 400 ± 50 pc from the Sun. Out of 13 confirmed members, only 5 single stars have been found. Its estimated present-day binary fraction is at least 62%. The calculated heliocentric space motion of the cluster is not compatible with possible membership in the Hyades stream.

Conclusions. Our results show that NGC 1901 is a clear prototype of open cluster remnant characterized by a large value of the binary fraction and a significant depletion of low-mass stars. In the light of numerical simulations, this is compatible with NGC 1901 being what remains of a larger system initially made of 500-750 stars.

Key words. open clusters and associations: individual: NGC 1901 – open clusters and associations: general

1. Introduction

Observations strongly suggest that present-day star formation in the Milky Way disk takes place in stellar clumps rather than in isolation. These stellar aggregates form out of giant molecular clouds and, in principle, they can be born bound or unbound. Unbound, short lived (< 50 Myr) stellar ensembles are called associations; bound, long lived stellar groups are known as open clusters. On the other hand, simulations show that open clusters can also be formed out of the remains of rich stellar associations (Kroupa et al. 2001).

As most of the field stars have been formed in the so-called clustered mode (i.e., in clusters or associations), not in the dispersed mode (i.e., in isolation), it is natural to identify these stellar clumps as the *de facto* units of star formation in the Galactic disk (Clarke et al. 2000). The idea of open clusters being fundamental units of star formation is, however, controversial (Meyer et al. 2000) as it has been argued that bound open clusters cannot contribute significantly to the field star population because they are rare and long lived (e.g. Roberts 1957). In contrast, most young embedded clusters are thought to evolve into un-

bound stellar associations, which produce the majority of stars that populate the Galactic disk (Lada & Lada 1991).

N -body simulations show that the dynamical evolution of open star clusters is mainly the result of encounters among cluster members, stellar evolution, encounters with giant molecular clouds, and the effect of the Galactic tidal field. They gradually lose stars as they evolve and in their final evolutionary stages they are disrupted, leaving a cluster remnant (OCR, e.g. de la Fuente Marcos 1998) made of a few stars. For a given Galactocentric distance, the distinctive features of these ghostly objects depend upon the original membership of the cluster, the fraction of primordial binaries (PBs), and the initial mass function. The outcome of these numerical simulations shows a relatively large (about 20%) percentage of binaries in OCRs of models without PBs and up to 80% for models with significant fraction of PBs (30%). The effects of preferential evaporation of low-mass stars in simulated OCRs are also quite important, with a significant depletion of the primordial low-mass stellar (or substellar) population compared to the group of more massive stars. The different evolutionary status characteristic of classical open clusters and their remnants can be traced in both their stellar composition and structural parameters, particularly

the degree of core-halo differentiation, that is larger in evolved objects. Simulations can also provide information on the correlation between cluster life-times and their primordial properties, like membership. Averaging cluster life-times for entire sets of numerical models (de la Fuente Marcos & de la Fuente Marcos 2004) as a function of N the following power law is obtained: $\tau = 0.011 N^{0.68}$ (in Gyr) with a correlation coefficient of $r = 0.995$ and associated errors in τ of $\sim 10\%$. This slope is very similar to the slopes found by Baumgardt (2001) and Baumgardt & Makino (2003) although the details of the simulations are rather different.

Although the dynamical evolution of open star clusters has been well studied and our degree of understanding on the various evolutionary stages turning cluster members into field population is satisfactory, the topic of detection of open cluster remnants is still controversial, not only because their intrinsic observational properties make them difficult to identify but also because there are no reliable classification criteria. In fact, the main question still is, in general, when does a star cluster become a cluster remnant? A first attempt to provide an answer to this important question can be found in Bica et al. (2001). In their work, they assume that a cluster becomes significantly depopulated and shows signs of being a remnant after losing 2/3 of its initial population and they suggest the acronym POCR (Possible Open Cluster Remnant) for a number of candidates. The application of this criterion to simulated clusters is quite straightforward, but it is difficult to use with real clusters mainly because star counts are incomplete and there is no observational method to provide a reliable estimate of the initial population of a given cluster. Unfortunately, simulations and observational results both suggest that membership is not the best criteria to determine if a dynamically evolved open cluster is an OCR. In order to detect an OCR, certain contrast of the candidate object against the stellar background is required. To be identified initially as stellar overdensity, a cluster must have a stellar density (or, more properly, a surface luminosity) larger than the local Galactic value. Simulations suggest that, for poorly populated open clusters, and before losing 2/3 of their initial population, the stellar density has become lower than the surrounding field and the resulting object can no longer be considered a remnant but some type of stellar stream (proper motions of the member stars remain similar although no overdensity can be recorded). For the Solar Neighbourhood, the stellar density of the system should be greater than $0.044 M_{\odot} \text{pc}^{-3}$. Moreover, the density of a star cluster in the Solar Neighbourhood must be greater than about $0.08 M_{\odot} \text{pc}^{-3}$ in order to be stable against tidal disruption. Taking these constraints into consideration, the smallest OCRs from poorly populated clusters ($N \leq 100$) should contain more than 40% of their initial population in order to have a stellar density larger than the surrounding field. This value is close to the one quoted in Bica et al. (2001) but the situation appears to change dramatically for richer clusters. OCRs from clusters having N in the range 200-500 should retain 10-20% of their initial members. For N in the range 750-1,000, they should keep about 7% of their initial population. Densely populated clusters ($N = 10,000$) generate OCRs containing about 0.1% of their initial population, but with stellar density in the range $0.3\text{-}15 M_{\odot} \text{pc}^{-3}$. OCRs from rich clusters are very different from those resulting from the evolution of small clusters. The surviving stellar system is the outcome of a long-term contest for dynamical stability and, typically, only highly stable hierarchical multiple systems are present there. They are the result of Gyrs of dynamical evolution.

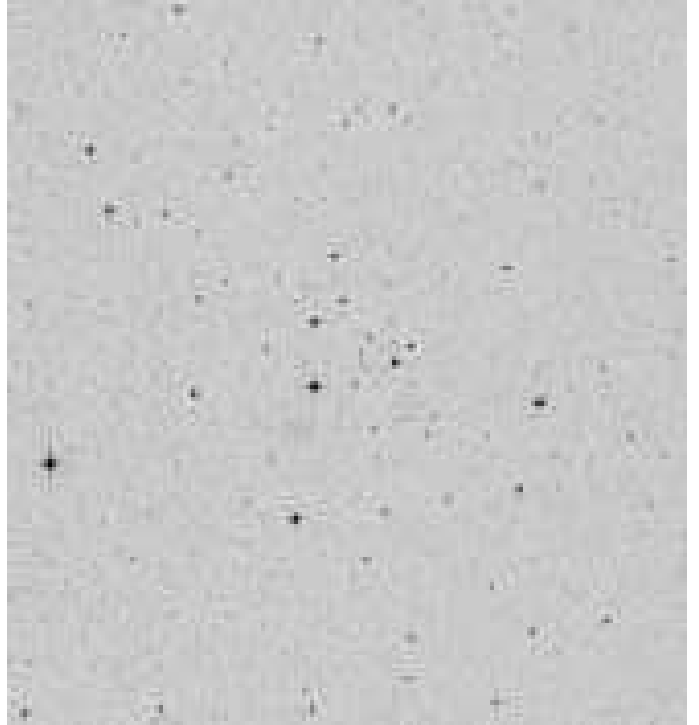


Fig. 1. DSS image of the area covered by the present study. North is up, east to the left, and the image is 20 arcmin on a side.

Observationally, Bica et al. (2001) selected 35 groups that stand up against the mean Galactic stellar fields, and are located relatively high onto the Galactic plane. Regrettably, the close scrutiny of the kinematics in some of them (Villanova et al. 2004a; Carraro et al. 2005; Carraro 2006) has shown that the contrast criterion is necessary but not sufficient to detect a remnant. In fact, when dealing with the remnant of a physical group, one expects that the remains itself exhibits all the features of a physical group. Following Platais et al. (1998), we define a physical group (at odds with a random sample of field stars) as an ensemble of stars which (1) occupy a limited volume of space, (2) individually share a common space velocity, and (3) individually share the same age and chemical composition, producing distinctive features in the H-R diagram.

In an attempt to provide tight observational constraints for numerical models, we have studied in detail the star group NGC 1901, which appears to be a promising open cluster remnant candidate. In this paper, we present new CCD UBVI photometry and 3 epoch spectroscopy, which we combine with proper motions from the UCAC2 catalog (Zacharias et al. 2004), with the aim to clarify the nature and dynamical status of this cluster. In Sect. 2 we provide a historical overview of the various analyses carried out previously for this object. Observations, data reduction, and overall results are presented in Sect. 3. In Sect. 4 we analyse proper motions and in Sect. 5 we discuss cluster members. In Sect. 6 we derive cluster fundamental parameters. Section 7 is devoted to identify possible fainter members. The current dynamical status is analysed in Sect. 8 and the connection with the Hyades stream is considered in Sect. 9. In Sect. 10 we draw some conclusions and suggest further lines of research.

2. Historical overview

The star group NGC 1901 was discovered in 1836 by J. F. W. Herschel but first noticed as a possible physical group by Bok & Bok (1960) while re-defining the van Wijk (1952) photometric sequence in front of the Large Magellanic Cloud (LMC). Bok & Bok (1960) emphasize that the region of the van Wijk sequence possibly represents a loose association of stars projected against the Large Cloud, since in this direction ($\alpha = 05^{\text{h}} 18^{\text{m}} 11^{\text{s}}$, $\delta = -68^{\circ} 27'$, $l = 279^{\circ}.03$, $b = -33^{\circ}.60$, J2000) the LMC is not very dense.

The photoelectric BV photometry collected by Sanduleak & Philip (1968, hereinafter SP68) allowed indeed to find out for the first time that the stars in the association compose a sequence in the Color Magnitude Diagram (CMD), compatible with a group of stars at 330 pc from the Sun. This result was noticed to be reinforced by the preliminary objective-prism radial velocities taken a few years before by Fehrenbach (1965), which showed how a few stars did have radial velocities smaller than the expected value (larger than 275 km s^{-1}) for objects belonging to the LMC. For some of these stars, SP68 provided proper motions from a variety of sources, showing that a substantial fraction of them did share common motion. A more detailed proper motion analysis was performed the same year by Murray et al. (1969), which confirmed the reality of the group but put it a 480 pc from the Sun, and called the attention to a possible dynamical relation with the Hyades, due to the very similar space motion components of the two groups. This argument has been thoroughly investigated by Eggen (1996), who found that the two systems are part of the Hyades stream. He found two separate kinematic groups that he called superclusters within the Hyades stream: the Hyades and the NGC 1901 superclusters. Using the UVW system defined in Sect. 9 the heliocentric space motion of the Hyades group is $(U, V, W) = (-40.4, -16.0, -3.0) \text{ km/s}$ and the equivalent result for the NGC 1901 group is $(U, V, W) = (-26.4, -10.4, -1.5) \text{ km/s}$. Although these results strongly suggest that two different kinematic structures are being observed, no discussion of errors or dispersions is given in Eggen's paper. Using samples observed by the Hipparcos satellite, Dehnen (1998) confirmed the present of two distinct moving groups in the area. The Hyades group was characterized by $(U, V, W) = (-40, -20, 0) \text{ km/s}$ and for the NGC 1901 group he found $(U, V, W) = (-25, -10, -15) \text{ km/s}$. Chereul et al. (1999) give $(U, V, W) = (-32.9, -14.5, -5.6) \text{ km/s}$ with velocity dispersions $(\sigma_U, \sigma_V, \sigma_W) = (6.6, 6.8, 6.5) \text{ km/s}$ for the Hyades group although they found three different groups within the supercluster. The NGC 1901 group is found at $(U, V, W) = (-26.1, -7.6, -0.7) \text{ km/s}$ with velocity dispersions $(\sigma_U, \sigma_V, \sigma_W) = (2.1, 3.7, 3.2) \text{ km/s}$. Again, both kinematic structures appear well separated.

Finally, a new investigation has been recently published by Pavani et al. (2001, hereinafter P01). They extended the photometry in a small area down to $V = 16$. However, the poor quality of the photometry and the lack of any new kinematic information prevented them from adding new pieces of information.

3. Observational material: Photometry

U, B, V , and I images centered on NGC 1901 were obtained at the Cerro Tololo Inter-American Observatory 1.0 m telescope, which is operated by the SMARTS¹ consortium. The telescope is equipped with a new $4k \times 4k$ CCD camera having a pixel scale of $0''.289/\text{pixel}$ which allows one to cover a field of $20' \times 20'$.

Table 1. Journal of photometric observations of NGC 1901 and standard star fields together with calibration coefficients (November 29, 2005).

Field	Filter	Exposure time [sec.]	Seeing	Airmass [ν]
NGC 1901	U	1200,60,5	1.1	1.150-1.280
	B	900,30,3	1.0	1.150-1.280
	V	600,30,1	1.0	1.150-1.280
	I	600,30,1	1.0	1.150-1.280
TPhoenix	U	180,200	1.0	1.024,1.444
	B	90,120	1.1	1.023,1.447
	V	20,30	1.1	1.024,1.450
	I	40,40	1.1	1.022,1.452
PG 0231+006	U	200,240	1.1	1.291,1.801
	B	60,90	1.1	1.293,1.807
	V	40,40	1.1	1.296,1.809
	I	40,30	1.1	1.294,1.810
Rubin 149	U	180,240	1.0	1.311,1.651
	B	90,120	1.1	1.316,1.649
	V	30,40	1.0	1.318,1.647
	I	40,40	1.0	1.313,1.643
Calibration coefficients		$u_1 = +3.285 \pm 0.004$		
		$u_2 = +0.032 \pm 0.006$		
		$u_3 = +0.46$		
		$b_1 = +2.188 \pm 0.004$		
		$b_2 = -0.160 \pm 0.006$		
		$b_3 = +0.27$		
		$v_{1bv} = +2.188 \pm 0.014$		$i_1 = +2.789 \pm 0.044$
		$v_{2bv} = +0.017 \pm 0.018$		$i_2 = +0.021 \pm 0.043$
		$v_3 = +0.12$		$i_3 = +0.06$
		$v_{1vi} = +2.188 \pm 0.016$		
	$v_{2vi} = +0.013 \pm 0.016$			

Observations were carried out on November 29, 2005. Three Landolt (1992) areas (TPhoenix, Rubin 149, and PG 0231+006) were also observed to tie the instrumental magnitudes to the standard system. The night was photometric with an average seeing of 1.1 arcsec. Data have been reduced using IRAF² packages CCDRED, DAOPHOT, and PHOTCAL. Photometry was done employing the point spread function (PSF) method (Stetson 1987). The covered area is shown in Fig. 1, while Table 1 contains the observational log-book.

The calibration equations read:

$$u = U + u_1 + u_2(U - B) + u_3X \quad (1)$$

$$b = B + b_1 + b_2(B - V) + b_3X \quad (2)$$

$$v = V + v_{1bv} + v_{2bv}(B - V) + v_3X \quad (3)$$

$$v = V + v_{1vi} + v_{2vi}(V - I) + v_3X \quad (4)$$

$$i = I + i_1 + i_2(V - I) + i_3X \quad (5),$$

where $UBVI$ are standard magnitudes, $ubvi$ are the instrumental ones, X is the airmass and the derived coefficients are presented at the bottom of Table 1. As for V magnitudes, when B magnitude was available, we used expression (3) to compute them, elsewhere expression (4) was used. The standard stars in these fields provide a wide color coverage, with $-1.217 \leq (U - B) \leq 2.233$, $-0.298 \leq (U - B) \leq 1.999$, and $-0.361 \leq (V - I) \leq 2.268$. Aperture correction was estimated in a sample of bright stars, and then applied to all the stars. It amounted at 0.315, 0.300, 0.280 and 0.280 mag for the U, B, V and I filters, respectively.

We now compare our photometry with previous investigations. We restrict this comparison to the photoelectric photometry of

¹ <http://www.astro.yale.edu/smarts/>

² IRAF is distributed by NOAO, which is operated by AURA under cooperative agreement with the NSF.

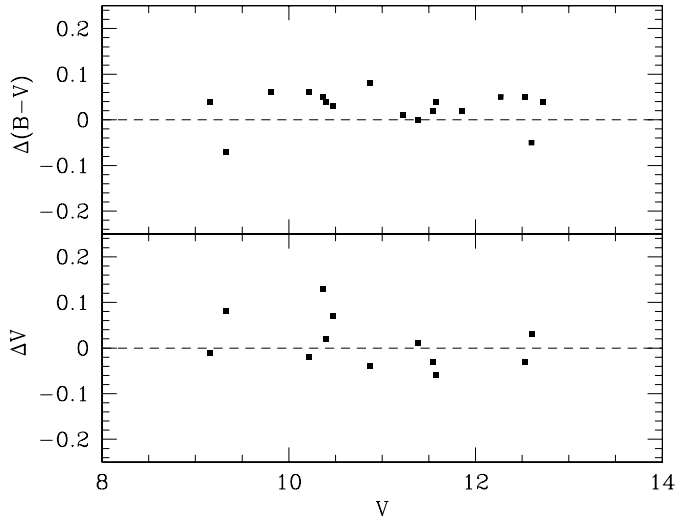


Fig. 2. Comparison with SP68 photoelectric photometry. The comparison is in the sense this study minus SP68

SP68 and the modern CCD study by P01. We have 12 stars in common with SP68, and the comparison in the sense this study minus SP68 reads:

$$\Delta(B - V) = 0.024 \pm 0.044 \quad (1)$$

$$\Delta V = 0.012 \pm 0.056 \quad (2)$$

In general, this comparison is very good and it is shown in Fig. 2. Now we turn to the only previous CCD investigation by P01. We have 30 stars in common and the comparison in the sense this study minus P01 reads:

$$\Delta(B - V) = 1.972 \pm 4.075 \quad (3)$$

$$\Delta V = -0.267 \pm 0.619 \quad (4)$$

In Fig. 3 only a sub-sample of these 30 stars is shown. Clearly some errors occurred in P01 photometry. P01 photometry compares well with SP68 and the present study down to $V \sim 11.5$, then it starts deviating increasingly with respect to the present study. We notice that P01 failed to compare their photometry with two more stars they have in common with SP68 (GSC091200626 and GSC092100834). While the present study compares very well with SP68 also for these two stars, P01 shows significant deviations (up to 0.5 mag in V) for these two stars. The comparison with P01 is shown in Fig. 3. Another strange point is that P01 assign two entries to TYC-2883 and GCS 0916200883 (actually the same star, HD 269310), but provide for it two very discrepant values of the magnitude and color and different suggestions about the membership.

The CMD of all the stars measured in the field of NGC 1901 (see Fig. 1) is shown in Fig. 4. The present photometry goes 7 mag deeper than P01 and provides a larger wavelength baseline (from U to I). The CMD in Fig. 4 is in the V vs $B - V$ plane, to compare with previous studies. The objective is to extend NGC 1901

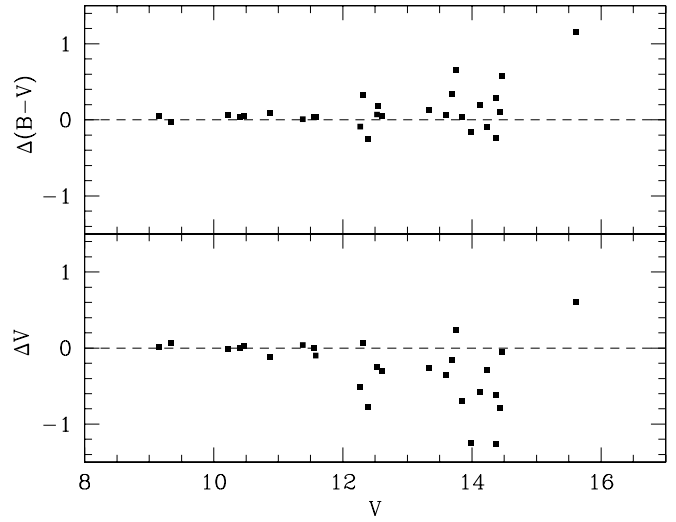


Fig. 3. Comparison with P01 CCD photometry. The comparison is in the sense this study minus P01. In this figure the two most deviating stars are not shown.

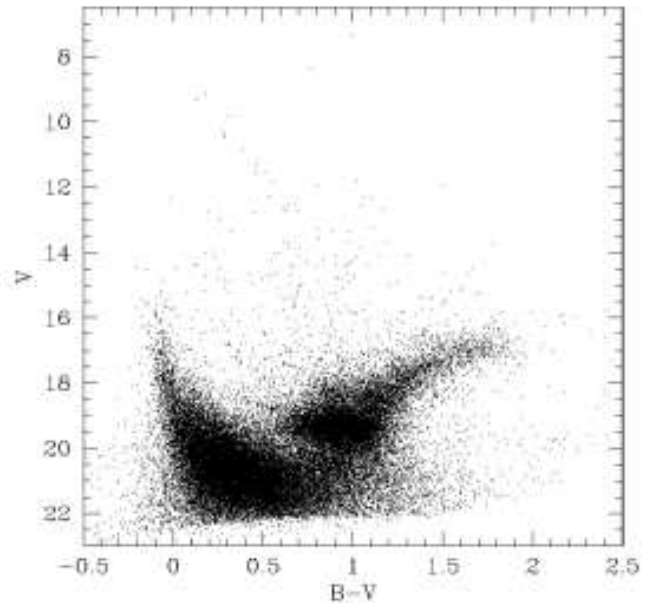


Fig. 4. BV CMD for all the stars detected in the present study having σ_B and σ_V smaller than 0.1 mag.

sequence as deep as possible. The main problem is, of course, the strong contamination from LMC stars. The LMC is dramatically visible in this CMD, with its young star Main Sequence (MS), intermediate-age population red clump, Asymptotic Giant Branch (AGB), and the older stars Red Giant Branch (RGB).

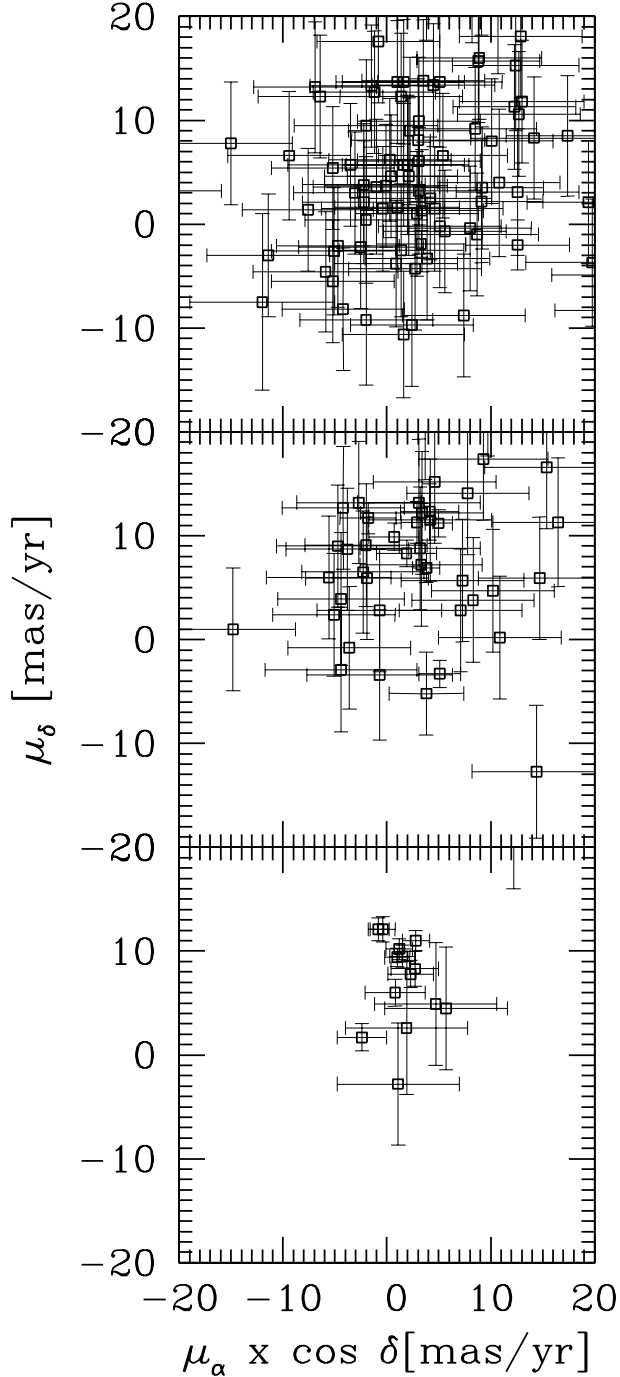


Fig. 5. Proper motion analysis. **Upper panel:** stars having $12 \leq K \leq 14$. **Middle panel:** stars having $10 \leq K \leq 12$. **Lower panel:** stars brighter than $K = 10.0$. These stars are used to search for a preliminary member list.

4. Proper motions

We have extracted the proper motion components in a 20 squared arcmin field around NGC 1901 from the UCAC2 catalogue (Zacharias et al. 2004), and constructed 3 vector point diagrams as a function of K magnitude (UCAC2 is in fact cross-correlated with 2MASS). The results are shown in Fig. 5, where the lower

panel is restricted to stars having $K \leq 10$, the middle panel to stars in the range $10 \leq K \leq 12$, and the upper panel to stars in the range $12 \leq K \leq 14$. The contamination from background stars is very high in the upper and middle panel. For this reason, we consider only the stars brighter than $K = 10$ (lower panel) to have an estimate of the cluster mean tangential motion and derive a first list of member candidates. In such way we extracted 35 stars from the catalog, from which we derived :

$$\mu_{\alpha} = 1.7 \pm 1.3 \text{ [mas/yr]} \quad (5)$$

$$\mu_{\delta} = 12.3 \pm 2.9 \text{ [mas/yr]} \quad (6)$$

Clearly, stars in the lower panel seem to visually clump around these values. Starting from here, we are going to consider proper motion probable members all the stars having proper motion component compatible within 2σ of these values.

5. Observational material: Spectroscopy

To obtain more solid information about the membership and dynamical status of NGC 1901 we carried out a multi-epoch spectroscopic campaign. With the aim to measure radial velocity and detect unresolved binaries, spectroscopy has been obtained during three different runs in 2002, 2003 and 2005.

5.1. La Silla data

The first epoch of radial velocity observations was already described in Villanova (2003) and Villanova et al. (2004b) and were carried out on the night of 2002 December 10 at the La Silla Observatory (ESO, Chile) under photometric conditions and a typical seeing of 1 arcsec. The EMMI spectrograph on the NTT 3.5-m telescope was used with a $1.0''$ slit to provide a spectral resolution $R = 33000$ in the wavelength range $3800\text{-}8600 \text{ \AA}$ on the two 2048×4096 CCDs of the mosaic detector. For the wavelength calibration, a single spectrum of a thorium-argon lamp was secured at the end of the night because of the stability of the instrument. The typical signal-to-noise of the spectra range from 70 to 170.

5.2. CASLEO data

This observational dataset consists of 4 high resolution spectra for radial velocities determination and 2 low resolution spectra for MK classification. The 4 high resolution spectra have been obtained in December 11-15, 2003 with the Echelle REOSC Cassegrain spectrograph attached to the 2.15m reflector at the Complejo Astronomico El Leoncito (CASLEO³), using a TEK 1024×1024 pixel CCD as detector. The spectra cover an approximate wavelength range from 3600 to 6000 \AA , at a reciprocal dispersion of $\sim 0.15 \text{ \AA}$ per pixel at 4000 \AA . Comparison arc images were observed at the same telescope position as the stellar images immediately before and after the stellar exposures. Spectra were all reduced using available IRAF routines. The radial velocities were determined on spectra normalized to the continuum, fitting Gaussian profiles to the observed line using IRAF routines, measured the position of the line or the two components presents in the echelle spectra. The 2 low resolution spectra observed from CASLEO, in December 8, 2004 with the

³ CASLEO is operated under agreement between CONICET, SECYT, and the National Universities of Cordoba, La Plata and San Juan, Argentina.

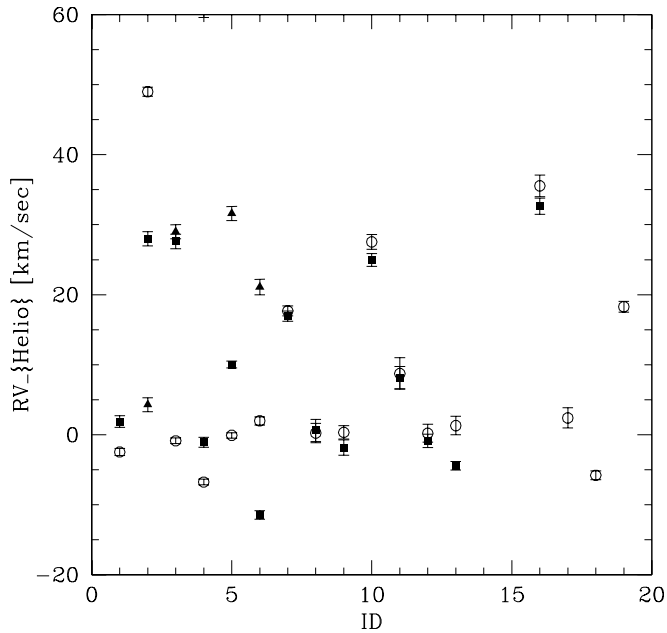


Fig. 6. Radial velocity distribution. Open circles indicate RVs from the Las Campanas run, filled squares indicate RVs from the La Silla run, and filled triangles the Casleo run.

same REOSC spectrograph as echelle but in its simple dispersion mode, provides on the TEK 1024×1024 a sampling of 1.64 Å per pixel, covering a wavelength range from 3900 to 5500 Å, over the classical range for MK classification. All spectra were reduced using standard IRAF routines.

5.3. Las Campanas data

The third epoch radial velocity observations were carried out on the nights of 2005 October 18-22 at the du Pont 2.5-m telescope at Las Campanas Observatory under variable photometric conditions and a typical seeing around 1 – 2". The echelle spectrograph was used with a 0.7" slit to provide a spectral resolution $R = 64000$ in the wavelength range 3600-10400 Å on the 2048×2048 CCD. Images were reduced using IRAF including bias subtraction, flat-field correction, extraction of spectral orders, wavelength calibration, sky subtraction, and spectral rectification. The single orders were merged into a single spectrum. The typical signal-to-noise of the spectra ranges from 50 to 80. The radial velocities of the target stars in the La Silla and Las Campanas runs were measured using the IRAF `fxcor` task, which cross-correlates the object spectrum with the template. The peak of the cross-correlation was fitted with a Gaussian curve after rejecting the spectral regions contaminated by telluric lines ($\lambda > 6850\text{Å}$). As templates we calculated a set of spectra covering all the T_{eff} range (4500-9000 K) of our stars using SPECTRUM, the Local Thermodynamical Equilibrium (LTE) spectral synthesis program freely distributed by Richard O'Gray⁴.

The obtained radial velocities for the three epochs are reported in Table 2 together with their errors, and plotted in Fig. 6.

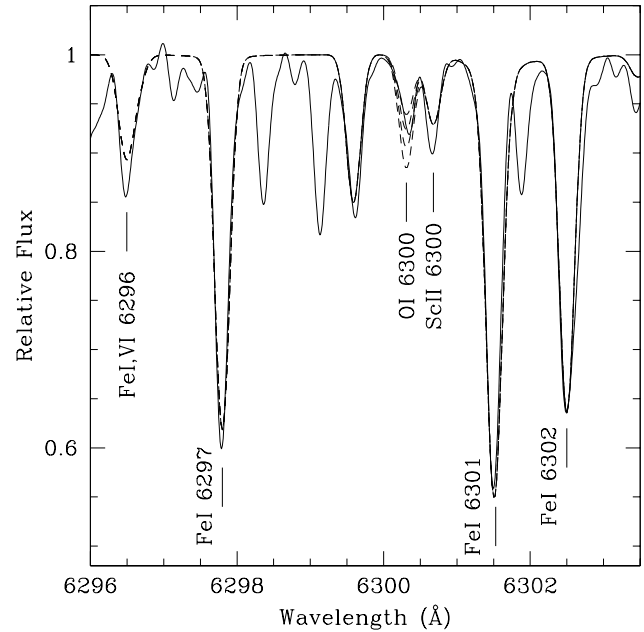


Fig. 7. Oxygen synthesis around 6300 Å region. The oxygen abundance covers the range from -0.2 dex (upper dashed line at 6300 Å) to +0.1 dex (lower dashed line at 6300 Å).

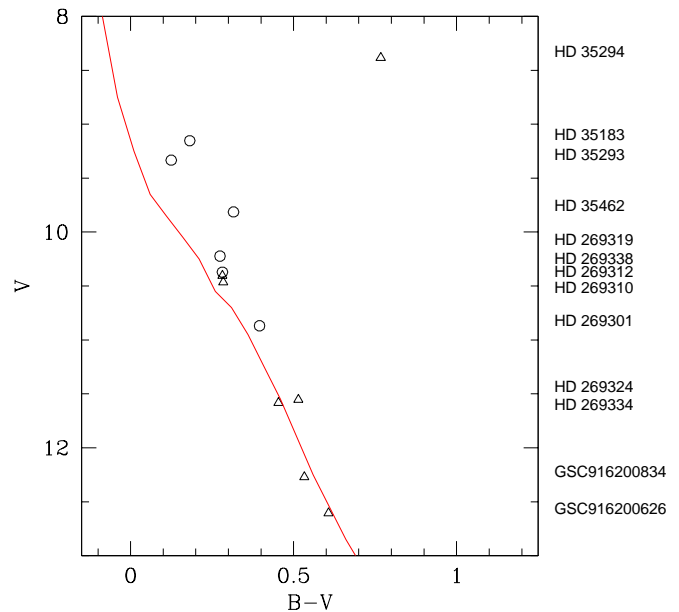


Fig. 8. Color Magnitude Diagram for cluster members. Circles indicate binaries, while triangles indicate single stars.

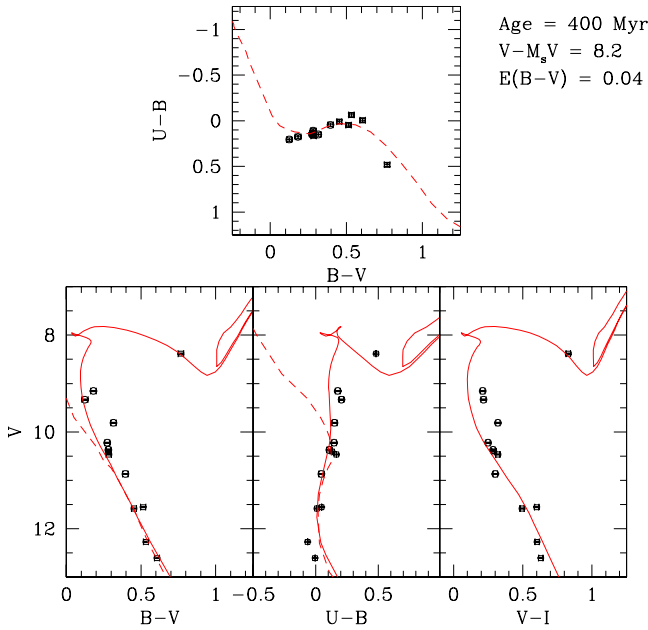
6. Cluster members

In this Section we make use of the stellar radial velocities, proper motions and positions in the various photometric diagrams to deem out interlopers and pick up cluster members. We consider here at first only the stars which have radial velocity, proper motion and multicolor photometry. With these stars we try to define the cluster MS, in order to be able later on to detect

⁴ www.phys.appstate.edu/spectrum/spectrum.html

Table 2. Basic data of suspected NGC 1901 members. In the last column M indicates membership to NGC 1901, NM no membership.

ID	Designation	α	δ	U	B	V	I	μ_α	μ_δ	RV_{Dic02}	RV_{Dic03}	RV_{Oct05}	$SpectralType$	Membership
		hh:mm:sec	o:m:s	mag	mag	mag	mag	mas/yr	ms/yr	km/sec	km/sec	km/sec		
2	HD35294	05:18:03.258	-68:27:56.69	9.63	9.15	8.38	7.55	1.0±1.2	9.4±0.9		4.3±1.0	2.4±1.4	G2IV	M
3	HD35183	05:17:23.034	-68:28:19.12	9.51	9.33	9.15	8.94	1.5±1.2	9.5±1.1	1.8±0.8	29.0±1.0	-2.5±0.5	A3V	M
4	HD35293	05:18:02.089	-68:21:19.48	9.66	9.46	9.33	9.12	-0.8±1.0	12.1±1.1	27.9±1.0	60.6±1.0	48.9±0.7	A1	M
5	HD35462	05:19:10.754	-68:34:51.72	10.28	10.13	9.81	9.49	1.2±1.3	10.2±1.0		31.6±1.0	18.3±0.8	A2V	M
6	HD269338	05:18:52.918	-68:34:13.35	10.76	10.65	10.37	10.08	-0.4±1.2	12.1±1.2		21.0±1.1	-5.8±0.6	A5	M
7	HD269319	05:18:22.479	-68:28:01.63	10.64	10.49	10.22	9.97	2.8±1.3	11.0±1.0	27.6±1.0		-0.9±0.4	A5	M
8	HD269312	05:18:11.983	-68:25:36.34	10.82	10.68	10.40	10.11	2.3±2.2	7.8±1.3	-1.1±0.7		-6.7±0.4		M
9	HD269310	05:17:59.168	-68:31:27.72	10.92	10.75	10.46	10.14	2.7±2.3	8.3±1.7	10.0±0.4		-0.1±0.4	A7V	M
10	HD269301	05:17:35.815	-68:21:47.16	11.31	11.26	10.87	10.56	5.0±1.3	11.2±1.3	-11.4±0.6		2.0±0.6	A9V	M
12	HD269315	05:18:16.683	-68:25:10.44	11.84	11.83	11.38	10.86	3.8±1.3	6.9±1.4	16.9±0.7		17.7±0.7	F5V	NM
13	HD269324	05:18:29.529	-68:27:13.81	12.11	12.07	11.55	10.95	2.9±1.5	11.3±2.0	0.6±1.6		0.2±1.4	F6V	M
14	HD269334	05:18:42.738	-68:27:32.76	12.04	12.03	11.58	11.09	1.9±2.9	8.3±1.3	-1.8±1.1		0.3±0.9	F3V	M
17	GSC916200464	05:18:27.560	-68:31:28.36	11.71	12.37	12.39	12.35	12.6±5.0	-2.0±2.4	268.6±1.6			G5V	NM
20	GSC916200834	05:19:05.214	-68:30:45.75	12.74	12.80	12.27	11.67	-1.8±2.7	11.7±1.5	-0.9±0.9		0.2±1.3	F8V	M
23	GSC916200682	05:18:41.691	-68:22:29.24	14.07	13.36	12.31	11.38	1.1±5.9	-2.8±5.9	8.2±1.6		8.7±2.2	K0	NM
25	GSC916201005	05:17:26.939	-68:25:41.23	13.32	13.16	12.53	11.79	1.6±5.9	30.4±5.9	24.9±0.9		27.5±1.0	F7	NM
27	GSC916200626	05:18:19.173	-68:26:25.15	13.21	13.21	12.60	11.97	0.7±2.4	9.9±1.3	-3.4±0.6		1.3±1.3	F8V	M
36	MACS0517684015	05:17:40.773	-68:29:04.73	14.52	14.22	13.34	12.35	10.3±5.9	32.6±5.9	32.6±1.1		35.5±1.5		NM
40	UCAC2-139	05:18:25.564	-68:17:19.25	14.48	14.37	13.74	12.96	-2.2±5.9	3.8±5.9	295.9±2.4		298.8±3.5		NM
41	GSC0916200216	05:17:51.066	-68:24:34.62	17.43	15.54	13.76	12.15	5.7±5.9	4.5±5.9	30.1±0.1		32.2±0.2		NM

**Fig. 9.** Color Magnitudes and Two Color Diagrams: looking for NGC 1901 fundamental parameters. The upper panel shows the TCD, while the three bottom panels shows the CMDs for different color combinations. The solid line in all the panels is the same isochrone shifted to fit the stars distribution, while the dashed line is the Schmidt-Kaler (1982) empirical ZAMS.

fainter photometric members along the extension of this MS. In the following we discuss the group membership on a star by star basis.

HD35294. This is a giant star of G2IV spectral type. Its radial velocity suggests that it is a single star and a member of NGC 1901. Fehrenbach & Duflot (1974) found similar values

for the radial velocity of this star, reassuring its single nature. Proper motions are also compatible with membership.

HD35183. This is clearly a binary star, but proper motions do suggest membership.

HD35293. This is another clear binary star, and again proper motions do suggest membership.

HD35462. Proper motions suggest that it is a member, but radial velocities seem to contradict this hypothesis. However, if we combine together our radial velocity measurements with older data (11 Km s^{-1} , Barbier-Brossat et al. 1994) it emerges that this is a binary star, therefore reinforcing the idea that it is a member of the group.

HD269338. This star is a binary, and proper motions and radial velocity are consistent with it being a cluster member.

HD269319. This star is a binary as well, and proper motions and radial velocity are consistent with it being a cluster member.

HD269312. Proper motions and radial velocity suggest this is a cluster member. This star has recently been studied by Cherix et al. (2006), who found that it is a δ Scuti variable candidate.

HD269310. This star is a binary, and proper motion and radial velocity identify it as a cluster member. Binarity is confirmed by Barbier-Brossat et al. (1994), who report values of -16 and 10 km/sec for this star.

HD269301. This star is a binary, and proper motion and radial velocity indicate that it is a cluster member.

HD269315. We propose this star is not a member. Radial velocity is significantly larger than the cluster average and proper motions also deviate from the mean tangential motion.

HD269324. Both radial velocity and proper motion indicate that this star is a member of NGC 1901.

HD269334. As in the previous case, both radial velocity and proper motion are suggesting that this star is a member of NGC 1901.

GSC0916200464. The high radial velocity, blue color and proper motion readily indicate that this is a LMC star.

GSC0916200834. This star is a clear member considering its proper motion and radial velocity.

GSC0916200682. P01 propose this is a member. However it looks a clear proper motion non-member, and the radial velocity confirms this conclusion.

GSC0916201005. Murray et al. (1969) already suggested that this is a non-member, although P01 propose it as a photometric member. Our radial velocity and UCAC 2 proper motions confirm Murray et al. results.

GSC0916200626. This star was found to be a proper motion non-member by Murray et al. (1969), but P01 include it among the list of probable cluster members. According to the UCAC2 proper motions, this is a likely member. Radial velocity is compatible with membership, although it may be a binary.

MACS0517684015. Both the radial velocity and proper motion of this binary demonstrate that it is a non-member.

UCAC2-139. The high radial velocity of this star suggests that it is a probable LMC member.

GSC0916200216. This is a single star for which both the radial velocity and the proper motion indicate it is an interloper.

7. NGC 1901 metal content

A chemical composition study of the cluster was performed by analyzing the spectrum of the star HD 35294, which we have shown to be a member. Being the coldest stellar member, it was the ideal target for this purpose. We used the equivalent widths method and measured the equivalent width of the spectral lines for the most important elements (O, Na, Mg, Si, Ca, Ti, Cr, Fe, Ni, Ba) using the standard IRAF routine `splot`. Repeated measurements show a typical error of about $5 m\text{\AA}$ for the weakest lines. The LTE abundance program MOOG (freely distributed by C. Sneden, University of Texas, Austin) was used to determine the metal abundances. Model atmospheres were interpolated from the grid of Kurucz (1992) models by using the values of T_{eff} and $\log(g)$ determined as explained below. Initial estimates of the atmospheric parameters (T_{eff} , $\log(g)$, and v_t) were obtained according to the spectral type of the star (G2IV). Then, during the abundance analysis, T_{eff} and v_t were adjusted to remove trends in abundances vs. excitation potential, and equivalent width for FeI lines in order to obtain better estimates. Besides, $\log(g)$ was adjusted in order to have the same abundance from FeI and FeII lines (ionization equilibrium). The final atmospheric parameters for HD 35294 are $T_{\text{eff}} = 5350 \pm 50\text{K}$, $\log(g) = 3.2 \pm 0.1$, and $v_t = 1.08 \pm 0.05 \text{ Km s}^{-1}$. The measured iron abundance is $[\text{Fe}/\text{H}] = -0.08 \pm 0.02$. Results for all the elements are reported in Table 3. The O content was determined

Table 3. NGC 1901 abundance analysis. NLTE correction is applied when necessary.

Element	LTE value	NLTE value
	dex	dex
[FeI/H]	-0.08±0.02	
[FeII/H]	-0.08±0.03	
[OI/H]7774	+0.05±0.09	-0.06±0.09
[OI/H]6300	-0.05±0.10	
[NaI/H]	-0.12±0.09	-0.02±0.09
[MgI/H]	-0.29±0.06	-0.13±0.06
[SiI/H]	-0.05±0.06	
[CaI/H]	-0.15±0.06	
[TiI/H]	-0.08±0.03	
[TiII/H]	-0.08±0.06	
[CrI/H]	-0.08±0.04	
[NiI/H]	-0.09±0.03	
[BaII/H]	+0.27±0.06	

using both the forbidden line at 6300 \AA and the permitted triplet at 7774 \AA . Because of blending with other spectral lines, abundance from the forbidden line was obtained comparing the observed spectrum with synthetic ones calculated for different O contents (see Fig 7 and Table 3). Na, Mg, and O are well known to be affected by NLTE effects. For this reason we applied abundance correction as prescribed by Gratton et al. (1999). Using these corrections, the O abundance obtained from the forbidden line (not affected by NLTE) agrees very well with the one obtained from the O triplet (affected by NLTE). The chemical composition shows a solar scaled mixture excepted for Ba, which is super-solar of about 0.35 dex. Also Na and Mg, using the NLTE corrections, are solar scaled as expected for a star cluster of this metallicity.

8. NGC 1901 reddening, distance and age

The CMD for the stars considered members of NGC 1901 is shown in Fig. 9 for various colour combinations. In Fig. 9 the Two Color Diagram is also shown. In this figure we superpose an isochrone of 400 Myr, for the exact metallicity, as derived in Section 7 for the star HD 35294. The value $[\text{Fe}/\text{H}] = -0.08$ translates into $Z = 0.016$ (Carraro et al. 1999). In the upper panel however, we simply superpose an empirical Zero Age Main Sequence (ZAMS) from Schmidt-Kaler (1982), shifted by $E(B - V) = 0.04 \pm 0.01$ ($E(U - B) = 0.029$). The same $E(B - V)$ and $E(U - B)$ are then used in the lower left and middle panel, respectively. Here, the isochrone is superposed together with the ZAMS, both shifted by $(V - M_V) = 8.2 \pm 0.1$. In the right panel, the isochrone and ZAMS are shifted by the same $(V - M_V)$ and by $E(V - I) = 0.05$. The fit is very good in all the diagrams, and from this we derive a distance of $400 \pm 50 \text{ pc}$ for NGC 1901. The reddening values we derived in different color indexes is compatible with a normal extinction law (Straižys 1992) toward the cluster. Starting from this point, we calculate the XYZ coordinates of NGC 1901 assuming 8.5 kpc for the distance of the Sun to the Galactic Center. We find that $X = 8.55 \pm 0.050$, $Y = 0.30 \pm 0.05$ and $Z = -0.220 \pm 0.05 \text{ kpc}$.

9. Searching for fainter members

We use the results of the previous section to search for possible fainter members for which no radial velocity information is available (see Table 4).

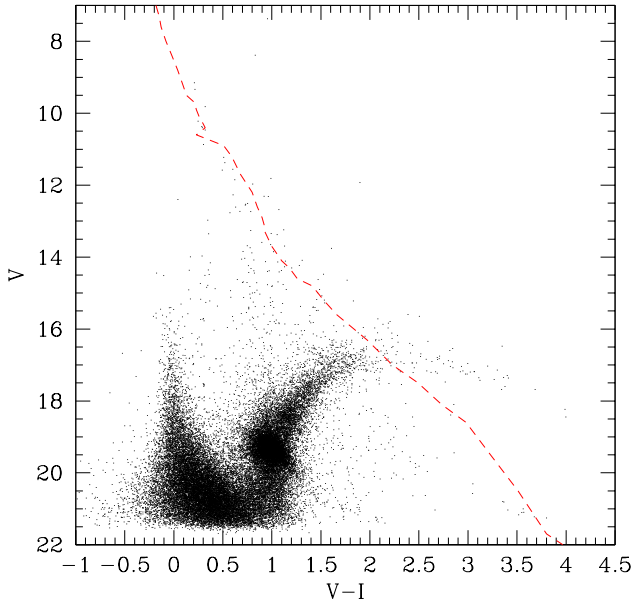


Fig. 10. Color Magnitude Diagram: searching for NGC 1901 faint members. The dashed line is a ZAMS shifted by the distance modulus and reddening derived in Section 8.

This is illustrated in Fig. 10, where the V vs $V-I$ CMD is shown. Here, only the stars with errors in V and $(V-I)$ lower than 0.1 are plotted. Basically, we search for faint members moving along the ZAMS, which is displaced by the same reddening and apparent distance modulus of above. We already have detected all the cluster members brighter than $V = 14$. Our objective is to look for stars close to the ZAMS (photometric probable members) which have as well proper motion components compatible with the bulk of the cluster members. This strategy works down to $V = 16$, which is the limit of the UCAC2 catalog. In the magnitude range $14 \leq V \leq 16$ we found only 3 more cluster possible members, namely # 34, 38, 93 (our numbering), but only one has compatible proper motion components. Some other stars, although close to the ZAMS (# 65, 70, 354 and 362), do possess incompatible proper motions, too. Below $V \approx 16$, the contamination of the RGB/AGB stars of the LMC makes it impossible to search for NGC 1901 cluster members. It is however possible that below the LMC RGB some M dwarfs members of NGC 1901 can be present ($V \approx 18$), simply looking at their position in the CMD. However, the lack of any kinematic information prevent us from assessing their membership in a reliable manner.

10. NGC 1901 Mass Function and dynamical status

Table 2 suggests that NGC 1901 has currently 13 members with $V < 13$. If we study the radial distribution of these likely members we obtain Fig. 11. The star density for a given value of the radius in pixels is calculated counting all the sources (members) enclosed by a circle of radius r and dividing by the area (πr^2) to obtain the surface density in stars/pixel². The final step in the reductions was to calculate the statistical mean error of the star density. If n stars are expected in an area A , samplings of independent areas of this size will give a Poisson distribution with mean error \sqrt{n} (King et al. 1968).

Figure 11 suggests that the effective radius of the cluster (including half the members) is about 650 pixels or 3.1 arcmin. For the adopted value of the distance, this translates into an effective radius of 0.4 pc. The tidal radius is defined as the distance from the cluster centre for which the relative acceleration becomes zero and it corresponds to the maximum distance that a star can reach without escaping from the cluster (e.g. Binney & Tremaine 1987). At the tidal radius the density distribution falls to zero. Following this criterion and from Fig. 11, the tidal radius can be estimated to be $r_t = 1.0$ pc (for a radius in pixels of 1800). The concentration parameter:

$$C = \log\left(\frac{r_t}{r_c}\right), \quad (7)$$

is a value commonly used to measure how centrally concentrated a cluster is. The core radius, r_c , is a well defined parameter of a King model (King 1962, 1966) but from a theoretical point of view it is not clear how it should be defined in situations, like the present one, in which a King model cannot be fit. On the other hand, the core radius as defined observationally is the radius at which the density distribution has fallen to just half the central density (for details see, e.g., Casertano & Hut 1985). In our case, it gives a value of 416 pixels or 0.23 pc. Therefore, the concentration parameter is rather low, about 0.64, that suggests a relaxed system with a rather small halo.

The current binary fraction of NGC 1901 is rather high, 8 binaries out of 13 confirmed members. This translates into a binary fraction close to 62%. In the classical paper by Duquennoy and Mayor (1991) about multiplicity in the Solar Neighborhood, they conclude that two thirds of the studied systems were multiples. This figure is very close to the value found in the cluster studied here. OCRs are expected to contain a higher than average fraction of multiple systems. Our results for NGC 1901 are not fully conclusive in this respect as are also compatible with the characteristic value of the multiple fraction for the local field population. If our estimate for the present-day binary fraction of this object is correct and we assume that it is a *bona-fide* OCR then simulations suggest that the primordial binary fraction for NGC 1901 was somewhat low, likely under 20%. On the other hand, our result can also be interpreted as evidence of actual incompleteness. It may be possible that a certain number of binaries remain hidden between the stellar contamination induced by the LMC and beyond $V = 13$. If true, this may contribute to underestimate the actual binary fraction. Fig. 10 appears to show a group of objects at $V \sim 21$ that may be cluster members.

The present-day mass function of NGC 1901 appears to be quite unusual. If we assume that Fig. 10 can be considered as representative of the CMD for this object, it is clear that the number of K and M stars is rather low. Although it could be the result of incompleteness, our analysis suggests that the scarcity of low-mass cluster members could be real, the result of dynamical evolution or preferential evaporation of low-mass stars.

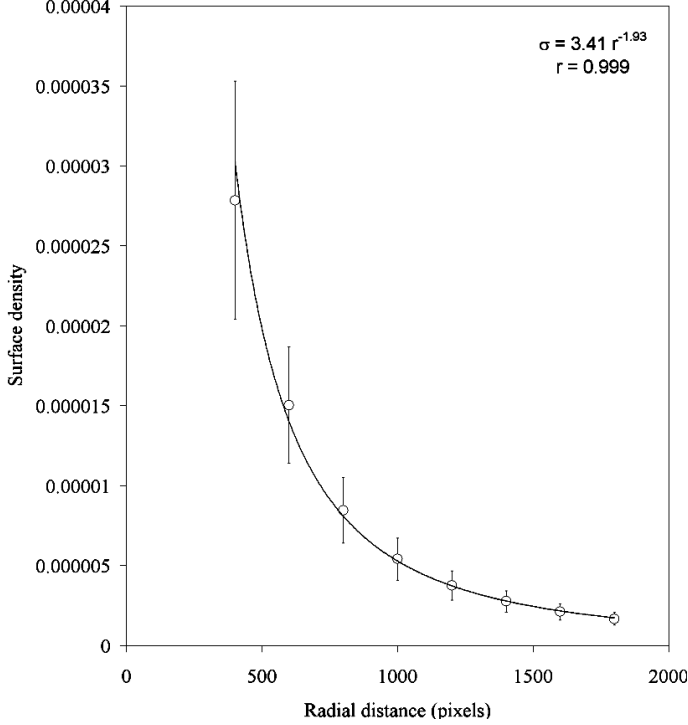
The initial mass function (hereafter IMF) or frequency distribution of stellar masses at birth (for a recent review on this subject see, e.g., Chabrier 2003, also Scalo 1986) is a fundamental parameter for studying the mass spectrum of open clusters. Salpeter (1955) used the observed luminosity function for the Solar Neighbourhood and theoretical evolution times to derive an IMF which may be approximated by a power-law:

$$n(M) \propto M^{-\alpha}, \quad (8)$$

where $n(M)$ is the number of stars per unit mass interval. The value of α is 2.35 for masses between 0.4 and 10.0 M_\odot . For the

Table 4. NGC 1901 additional probable members. In the last column, PM indicates probable members, PNM probable non-members.

ID	α	δ	U	B	V	I	μ_α	μ_δ	Membership
	hh:mm:sec	o:m:s	mag	mag	mag	mag	mas/yr	mas/yr	
34	05:17:05.811	-68:36:13.94	14.38	14.06	13.26	12.47	19.8±6.4	-3.7±6.1	PNM
38	05:17:51.366	-68:26:08.28	14.75	14.40	13.59	12.69	3.7±5.9	21.3±5.9	PM
65	05:17:56.494	-68:24:22.36	15.54	15.03	14.12	13.19	7.4±5.9	-8.8±5.9	PNM
70	05:20:02.775	-68:24:43.23	16.06	15.36	14.40	13.36	8.2±5.9	23.4±5.9	PNM
93	05:17:07.433	-68:34:40.54	16.48	15.77	14.76	13.64	-2.0±6.4	-9.2±6.3	PNM
354	05:19:51.456	-68:23:01.67	18.57	17.40	16.14	14.71	-5.2±5.9	29.2±5.9	PNM
362	05:17:00.535	-68:34:57.37	18.68	17.30	16.05	14.75	10.8±5.9	4.0±7.1	PNM

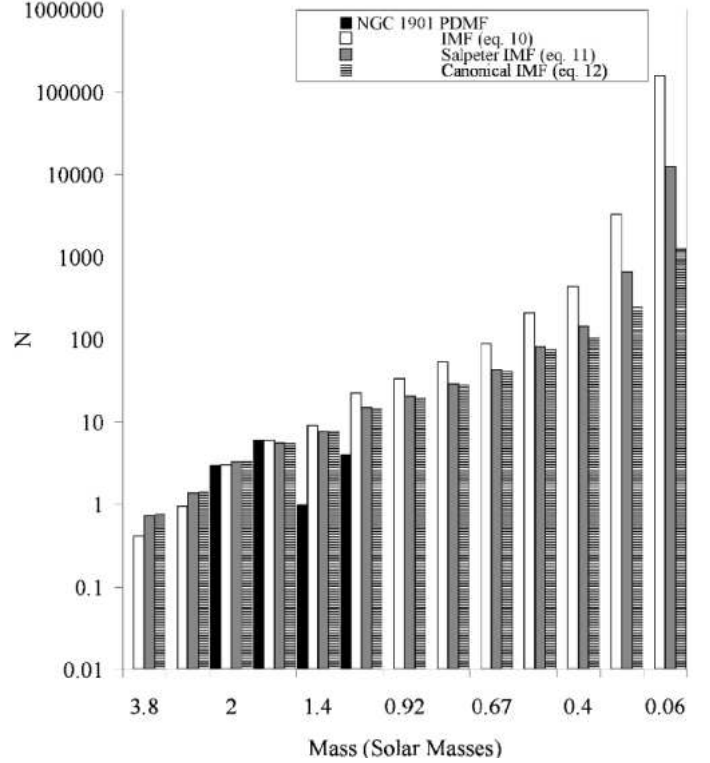
**Fig. 11.** Star counts of assumed NGC 1901 members as a function of radius.

particular case of open star clusters, Taff (1974) found different slopes in the range 2.50–2.74 depending on the concentration of stars at the center of the cluster, the contrast of the cluster with the surrounding stellar field –Shapley’s (1933) and Trumpler’s (1930) classifications– and the abundance of stars and range of brightness. The IMF in Taff’s work can be described by $\alpha = 2.50$ for clusters with $N \leq 100$ and $\alpha = 2.65$ for clusters with $N > 100$. Note however that the canonical IMF parametrization constitutes a two-part power-law IMF in the stellar regime (e.g. Pflamm-Altenburg & Kroupa 2006):

$$n(M) = k \begin{cases} (M/M_0)^{-\alpha_1} & M_0 \leq M < M_1, \\ (M_1/M_0)^{-\alpha_1} (M/M_1)^{-\alpha_2} & M_1 \leq M < M_{max}, \end{cases} \quad (9)$$

where M_0, M_1, M_{max} are equal to 0.08, 0.5, 150.0 M_\odot , respectively, and α_1, α_2 are 1.3, 2.3, respectively.

The present day mass function (hereafter PDMF) for main sequence stars in NGC 1901 after Table 2 is displayed in Fig. 12. It shows clear signs of incompleteness for spectral types later than A9. This could be a dynamical effect, the result of an increased escape rate for low-mass stars. It is well known that the dynamics of small and intermediate size clusters is dominated by relatively few heavy members. In the following we use the

**Fig. 12.** Observed present day mass function for NGC 1901 main sequence stars and various IMF fits. See the text for details.

heaviest main sequence members of the cluster to estimate the IMF of NGC 1901. In these calculations, we assume implicitly that the dynamical evolution of the cluster has not changed significantly the population of A stars and that the actual number of these stars has remained relatively unchanged since the cluster was formed. If we use the mass intervals [1.6, 2.0] and [2.0, 3.0] M_\odot (spectral types A9 to A5 and A4 to A0, respectively) to fit a simple power-law IMF we obtain

$$n(M) = (26 \pm 24) M^{-(3.1 \pm 1.1)}. \quad (10)$$

The result is displayed in Fig. 12. This IMF produces an initial cluster with a total mass of 10,600 M_\odot and almost 30,000 members. This result clearly overestimates the initial number of low-mass stars in the cluster. On the other hand, if we fit the data to a Salpeter IMF we obtain

$$n(M) = (16.7 \pm 1.4) M^{-2.35}. \quad (11)$$

This IMF (see Fig. 12) produces a cluster with an initial mass of 1,100 M_\odot and about 2750 members. This is likely also an

overestimate. Our best result is obtained for a canonical two-part power-law IMF:

$$n(M) = \begin{cases} (33 \pm 4) M^{-1.3} & 0.08 \leq M < 0.5, \\ (16.3 \pm 1.4) M^{-2.3} & 0.5 \leq M < 9, \end{cases} \quad (12)$$

The result is displayed in Fig. 12. For this IMF, the initial total mass of the cluster is $328 M_{\odot}$ with about 820 initial members (estimated errors of 10%). This is fully consistent with results for the life-time of 750-1000 members simulated clusters (e.g. de la Fuente Marcos, 1997).

The present-day integrated visual magnitude of the cluster can be estimated using the expression

$$M_V - M_V^{\odot} = -2.5 \log \frac{\Sigma L_i}{L_{\odot}}, \quad (13)$$

where M_V is the integrated absolute visual magnitude of the cluster, M_V^{\odot} is the solar equivalent, $L = \Sigma L_i$ is the total luminosity of the cluster, and L_{\odot} is the solar luminosity. The present day integrated absolute visual magnitude of NGC 1901 including all the members in Table 2 is -0.4, far from the value of the Hyades, -2.7, as expected. On the other hand, if we use our best result for the IMF, the initial integrated magnitude could have been as high as -1.4.

11. NGC 1901 motion

We derive here NGC 1901 kinematics by considering the 6 *bona fide* single star members. We obtain

$$RV = 0.50 \pm 0.48 [km/sec]$$

This is derived averaging two epochs RVs, when available, and then deriving the weighted mean of the five stars.

$$\mu_{\alpha} \times \cos \delta = 1.8 \pm 1.5 [mas/yr]$$

$$\mu_{\delta} = 10.7 \pm 1.7 [mas/yr]$$

These values show a very good match with Baumgardt et al. (2000).

In order to calculate the Galactic space velocity of this object and its uncertainty, we average the heliocentric Galactic velocity components for the five suspected single stars that have been considered as likely members in Sect. 6, namely stars 2, 13, 14, 20 and 27. These calculations have been carried out as described in Johnson and Soderblom (1987) for equinox 2000. Our results are referred to a right-handed coordinate system so that the velocity components are positive in the directions of the Galactic center, U, Galactic rotation, V, and the North Galactic Pole, W. We use the value of the parallax associated to the value of the distance determined in Sect. 8 and its error. Results are displayed in Table 5. They are based on relative proper motions, not absolute ones.

From these values, we derive the Heliocentric reference frame velocity UVW, which turn out to be $U = -19.0 \pm 1.2$ km/s, $V = -1.6 \pm 0.8$ km/s and $W = -2.7 \pm 0.7$ km/s. This yields a total velocity $V_T = 19.3$ km/s. The standard deviations are $\sigma_U = 6.7$ km/s, $\sigma_V = 2.9$ km/s and $\sigma_W = 1.5$ km/s. If only four stars are considered (star 27 could be a long-period binary) our results are $U = -19.0 \pm 1.5$ km/s ($\sigma_U = 8.9$ km/s), $V = -1.9 \pm 0.9$ km/s ($\sigma_V = 1.8$ km/s), and $W = -2.9 \pm 0.8$ km/s ($\sigma_U = 1.6$ km/s), then $V_T = 19.3$ km/s. These values are not in reasonable agreement with Eggen (1996), Dehnen (1998) and Chereul et al. (1999).

In principle one may argue that using relative proper motions may be a major factor in accounting for this lack of agreement. SIMBAD lists proper motions from the Tycho Reference Catalogue (Hog et al., 1998) for seven members (HD35294, HD35293, HD35462, HD269338, HD269319, HD269310 and HD269301). The values provided by this catalogue agree very well with the ones used in this paper; therefore, the observed discrepancies have not been originated by the proper motions used. On the other hand, HD 35183 has parallax and proper motions in the Hipparcos Catalogue (Perryman et al., 1997). Using the values provided by this catalogue ($d = 820 \pm 584$ pc, $\mu_{\alpha} = 1.07 \pm 1.03$ mas/yr, $\mu_{\delta} = 10.97 \pm 0.94$ mas/yr) and our average value for the radial velocity, we obtain for this star $U = -43 \pm 33$ km/s, $V = -3 \pm 3$ km/s and $W = -6 \pm 7$ km/s. This yields a total velocity $V_T = 43.5$ km/s. These numbers are much closer to the values usually quoted in the literature for the Hyades stream (see Sect. 2) but they are the result of using a value of the distance that is twice the one found in our study, even though they are still significantly different. We certainly believe that the value of the distance is the main source of discrepancies in this case. In any case, NGC 1901 is older than the Sirius supercluster (300 Myr) but younger than the Hyades supercluster (600 Myr).

12. Conclusions

We have presented a detailed photometric and spectroscopic study of the stellar group NGC 1901 with the aim to provide an observational template of a star cluster remnant to serve as example for theoretical investigations of star cluster evolution and dissolution.

The data we have acquired allow us to derive the following conclusions:

- we have identified 13 photometric, spectroscopic and astrometric members;
- these stars identify a stellar group at 400 pc from the Sun, and 400 million years old;
- within the errors of our spectroscopic campaign, out of 13 stars, 8 turn out to be binaries, which implies a binary fraction close to 62%; we suggest that this is only a lower limit.
- we found a prominent lack of M dwarfs and interpret this fact as the evidence that the group has lost most of its low mass members;
- we cannot confirm the possible kinematic association of NGC 1901 to the Stream I discussed in Eggen (1996);
- in the light of numerical simulations (de la Fuente Marcos 1998), this is compatible with NGC 1901 being what remains of a larger system initially made of 500-750 stars.

Finally, we would like to emphasize that future studies should be focused on better constraining the binary fraction of this stellar group. Probably a few more epochs should be sufficient to clarify the nature of all the doubtful cases.

Acknowledgements. The work of GC has been supported by *Fundacion Andes*. In preparation of this paper, we made use of the NASA Astrophysics Data System and the ASTRO-PH e-print server. This work made extensive use of the SIMBAD database, operated at the CDS, Strasbourg, France.

References

- Barbier-Brossat, M., Petit, M., & Figon, P. 1994, A&AS, 108, 603
 Baumgardt, H. 2001, MNRAS, 325, 1323
 Baumgardt, H., & Makino, J. 2003, MNRAS, 340, 227
 Baumgardt, H., Dettbarn, C., Wielen, R. 2000, A&AS, 146, 251

Table 5. Space motions of suspected single NGC 1901 members.

ID	Designation	α	δ	μ_α	μ_δ	U	V	W
		hh:mm:sec	°:′:″	mas/yr	mas/yr	km/sec	km/sec	km/sec
2	HD35294	05:18:03.258	-68:27:56.69	1.0±1.2	9.4±0.9	-17.2±5.9	-4.1±1.6	-4.2±2.2
13	HD269324	05:18:29.529	-68:27:13.81	2.9±1.5	11.3±2.0	-21.3±9.3	-2.6±1.7	-2.0±2.8
14	HD269334	05:18:42.738	-68:27:32.76	1.9±2.9	8.3±1.3	-15.8±6.5	-0.9±3.2	-1.0±4.7
20	GSC916200834	05:19:05.214	-68:30:45.75	-1.8±2.7	11.7±1.5	-21.8±8.3	-0.1±3.0	-4.3±4.4
27	GSC916200626	05:18:19.173	-68:26:25.15	0.7±2.4	9.9±1.3	-18.7±7.1	-0.3±3.3	-2.0±4.1

- Bica, E., Santiago, B. X., Dutra, C. M., Dottori, H., de Oliveira, M. R., & Pavani, D. 2001, *A&A*, 366, 827
- Binney, J., & Tremaine, S. 1987, *Galactic Dynamics* (Princeton: Princeton University Press)
- Bok, B. J., & Bok P. F. 1960, *MNRAS*, 121, 531
- Carraro, G. 2006, *BASI*, 34, 153
- Carraro, G., Girardi, L., & Chiosi, C. 1999, *MNRAS*, 309, 430
- Carraro, G., Dinescu, D. I., Girard, T. M., & van Altena, W. F. 2005, *A&A*, 433, 143
- Casertano, S., & Hut, P. 1985, *ApJ*, 298, 80
- Chabrier, G. 2003, *PASP*, 115, 763
- Chereul, E., Créz, M., Bienaymé, O. 1999 *A&AS*, 135, 5
- Cherix, M., Carrier, F., Burki, G., Blecha, A. 2006, *Mem. S. A. It.* 77, 328
- Clarke, C. J., Bonnell, I. A., & Hillenbrand, L. A. 2000, in *Protostars and Planets IV*, eds. Mannings, V., Boss, A. P., & Russell, S. S., University of Arizona Press, p. 151
- Dehnen, W. 1998, *AJ*, 115, 2384
- Duquenois, A., & Mayor, A. 1991, *A&A*, 248, 485
- Eggen, O. J. 1996, *AJ*, 111, 1615
- Fehrenbach, C. 1965, *Journal des Observateurs*, Vol. 48, p.199
- Fehrenbach, C., & Duflot, M. 1974, *A&AS*, 13, 173
- de la Fuente Marcos, R. 1997, *A&A*, 322, 764
- de la Fuente Marcos, R. 1998, *A&A*, 333, L27
- de la Fuente Marcos, R., & de la Fuente Marcos, C. 2004, *New Astronomy*, 9, 6
- Gratton, R. G., Carretta, E., Eriksson, K., & Gustafsson, B. 1999, *A&A*, 350, 955
- Hog, E., Kuzmin, A., Bastian, U., Fabricius, C., Kuimov, K., Lindegren, L., Makarov, V. V., & Roeser, S. 1998, *A&A*, 335, L65
- Johnson, D. R. H., & Soderblom, D. R. 1987, *AJ*, 93, 864
- King, I. R. 1962, *AJ*, 67, 471
- King, I. R. 1966, *AJ*, 71, 276
- King, I. R., Hedemann, E., Hodge, S. M., & White, R. E. 1968, *AJ*, 73, 456
- Kroupa, P., Aarseth, S. J., & Hurley, J. 2001, *MNRAS*, 321, 699
- Kurucz, R. L. 1992, in *The Stellar Population of Galaxies*, eds. Barbuy, B., Renzini, A., Kluwer, Dordrecht, p. 225
- Lada, C. J., & Lada, E. A. 1991, in *The Formation and Evolution of Star Clusters*, eds. Janes, K., ASP Conference Series, p. 3
- Landolt, A. U. 1992, *AJ*, 104, 340
- Meyer, M. R., Adams, F. C., Hillenbrand, L. A., Carpenter, J. M., & Larson, R. B. 2000, in *Protostars and Planets IV*, eds. Mannings, V., Boss, A. P., & Russell, S. S., University of Arizona Press, p. 121
- Murray, C. A., Dickens, R. J., & Walker, E. N. 1969, *Observatory*, 89, 104
- Pavani, D. B., Bica, E., Dutra, C. M., Dottori, H., Santiago, B. X., Carranza, G., & Diaz, R. J. 2001, *A&A*, 374, 554
- Perryman et al. 1997, *A&A*, 323, L49
- Pflamm-Altenburg, J., & Kroupa, P. 2006, *MNRAS*, 373, 295
- Platais, I., Kozhurina-Platais, V., & van Leeuwen, F. 1998, *AJ*, 116, 2423
- Roberts, M.S. 1957, *PASP*, 69, 59
- Salpeter, E. E. 1955, *ApJ*, 121, 161
- Sanduleak, N., & Philip A. G. D. 1968, *AJ*, 73, 566
- Scalo, J.M. 1986, *Fundam. Cosmic Phys.*, 11, 1
- Schmidt-Kaler, T. 1982, in *Landolt-Bornstein: Numerical data and Functional Relationships in Science and Technology*, vol 2b, eds. Schaifers, K., Voigt, H. H. (Springer: Berlin)
- Shapley H. 1933, *Star Clusters*, *Hdb. Astrophys.* 5/2
- Stetson, P. B. 1987, *PASP*, 99, 191
- Straizys, V. 1992, *Multicolor Stellar Photometry*, Pachart Publishing House, Tucson, Arizona
- Taff, L. G. 1974, *AJ*, 79, 11.
- Trumpler, R. 1930, *Lick Bull.* 14 Nr. 420
- Villanova, S. 2003, Master Thesis, Padova University
- Villanova, S., Carraro, G., de la Fuente Marcos, R., & Stagni, R. 2004a, *A&A*, 428, 67
- Villanova, S., Carraro, G., & de la Fuente Marcos, R. 2004b, *ASPC*, 317, 196
- van Wijk, U. 1952, *Harvard Bull.*, No. 921, 7
- Zacharias, N., Urban, S. E., Zacharias, M. I., Wycoff, G. L., Hall, D. M., Monet, D. G., & Rafferty, T. J. 2004, *AJ*, 127, 3043